A size-invariant bud-duration timer enables robustness in yeast cell size control

Corey A.H. Allard[1,2,†], Franziska Decker[1,3,†], Orion D. Weiner[1,4,*], Jared E. Toettcher[1,5,*], and Brian R. Graziano[1,4,6,*]

[1]Marine Biological Laboratory, Woods Hole, MA
[2]Dept. of Biochemistry and Cell Biology, The Geisel School of Medicine at Dartmouth, Hanover, NH 03755
[3]Max Planck Institute for the Physics of Complex Systems, Max Planck Institute of Molecular Cell Biology and Genetics, Center for Systems Biology Dresden, Dresden, Germany
[4]Cardiovascular Research Institute and Dept. of Biochemistry and Biophysics, UC San Francisco
[5]Department of Molecular Biology, Princeton University, Princeton, NJ
[6]Lead contact
†Co-first author
*Corresponding author

Corresponding Authors:

Brian Graziano
University of California, San Francisco
Cardiovascular Research Building, Room 384, MC 3120
555 Mission Bay Blvd. South
San Francisco, CA 94158
Tel. 617-501-3706
brian.graziano@ucsf.edu

Jared Toettcher
Lewis Thomas Laboratory Room 140
Washington Road
Princeton, NJ 08544
Tel. 609-258-1894
toettcher@princeton.edu

Orion Weiner
University of California, San Francisco
Cardiovascular Research Building, Room 352F, MC 3120
555 Mission Bay Blvd. South
San Francisco, CA 94158
Tel. 415-514-4352, Fax 415-514-1176
orion.weiner@ucsf.edu

ABSTRACT

Cell populations across nearly all forms of life generally maintain a characteristic cell type-dependent size, but how size control is achieved has been a long-standing question. Prior work has uncovered diverse size control strategies operating at distinct cell cycle stages, but it is unclear how these numerous pathways are integrated to provide robust, systems-level cell size control for any organism. Here, we probe cell growth and size control in budding yeast that can be reversibly blocked from bud initiation. While blocked, cells continue to grow isotropically, increasing their volume by more than an order of magnitude over unperturbed cells. Upon release, these 'giant' yeast resume budding and the population returns to its initial volume distribution within a few cell division cycles. Size control under these conditions does not require an explicit molecular size sensor. Instead, our observations are consistent with a size-invariant bud growth timer specifying the duration of S/G2/M to limit daughter cell size.

INTRODUCTION

Size is a fundamental property of cells that drives many key aspects of their physiology, including the abundance of organelles (Goehring and Hyman, 2012; Marshall, 2011) and DNA ploidy (Gregory, 2001). Maintenance of uniform size may also underlie the efficient functioning of tissues and organs (Ginzberg et al., 2015). In unicellular organisms such as the budding yeast (*S. cerevisiae*), individual cells in unperturbed populations have been observed to grow exponentially in size between birth and cell division (Elliott and McLaughlin, 1978; Godin et al., 2010; Soifer et al., 2016; Di Talia et al., 2007). However, exponential growth poses a problem in the presence of cell-to-cell growth variability as modeling has shown that it would amplify small size differences between newborn cells. Un-regulated exponential growth would thus lead to arbitrarily large and small cells in a population, in conflict with data showing that most cell types exhibit a narrow size distribution (Ginzberg et al., 2015).

To resolve the paradox between exponential single-cell growth and a narrow cell size distribution, it has been proposed that cells use various size-control strategies to counteract extreme size variation (Amodeo and Skotheim, 2016; Brooks and Shields, 1985; Ginzberg et al., 2015; Lloyd, 2013). These include (i) a 'sizer', where progression through the cell cycle is only triggered after cells surpass a specified size; (ii) an 'adder', where cells add a constant volume increment over the course of each cell cycle, dividing more rapidly if this increment is reached sooner; and (iii) the 'timer', where certain cell cycle phases exhibit a fixed duration, independent of cell size, to limit the extent of cell growth over these periods (Amir, 2014; Campos et al., 2014; Conlon and Raff, 2003; Fantes, 1977; Johnston et al., 1977; Pan et al., 2014; Taheri-Araghi et al., 2015; Varsano et al., 2017).

Quantitatively monitoring cell growth in yeast—as well bacterial, archaeal, and mammalian cells—show that the behavior of many organisms is consistent with an adder that monitors size across an entire cell cycle to correct for deviations in cell size and maintain size homeostasis in the population (Cadart et al., 2018; Eun et al., 2018; Soifer et al., 2016; Taheri-Araghi et al., 2015). Yet recent work suggests that at least for budding yeast, the observed adder actually arises as a phenomenological consequence of independent regulation of the pre- and post-Start cell cycle period (Chandler-Brown et al., 2017). According to this model, a sizer at the G1/S boundary halts the progression of small cells, allowing them to gain proportionally more volume than larger cells before progressing through Start into S-phase (Johnston et al., 1977; Schmoller, 2017; Schmoller

et al., 2015). Supporting this model, genetic perturbations that alter cell size leave the pre-Start sizer intact but remove the constant volume increment between cell generations predicted by the adder (Chandler-Brown et al., 2017). These studies also define a procedure for uncovering the underlying regulatory principles of size control: by perturbing cell size outside of its normal range and identifying invariant properties (e.g. minimum size in the case of a sizer; constant volume increment in the case of an adder), the key variables underlying its regulation can be uncovered.

However, the current model leaves many questions unanswered. First, size control is only well-described for small cells, but no mechanisms have been clearly defined to limit the growth of abnormally large cells. Nevertheless, many physiological perturbations can result in abnormally large cells (Hartwell and Unger, 1977; Spoerl et al., 1954), and mechanisms must also exist to ensure cells that grow too large can return to the set-point after successive rounds of growth and division. Underscoring the importance of this aspect of size homeostasis, tumor cells lacking functional size-homeostasis pathways often grow far larger than normal (Ginzberg et al., 2015). Second, in contrast to the pre-Start "sizer", there are conflicting data on post-Start regulation. The duration of budding in wildtype cells has been reported to only exhibit a weak dependence on cell size, so larger cells would be expected to add a larger volume than smaller ones (Charvin et al., 2009; Johnston et al., 1977; Di Talia et al., 2007). However, even large mother cells produce smaller daughters, suggesting that additional regulation may play a role during S/G2/M, either by limiting bud growth rate or shortening the duration of budding (Johnston et al., 1977). There is also conflicting evidence regarding the molecular size control mechanisms that might operate during S/G2/M, such as whether the kinase Swe1, the budding yeast homolog of fission yeast Wee1, regulates growth by sensing bud size or bud morphogenesis (Harvey and Kellogg, 2003; McNulty and Lew, 2005). Together, these data suggest that there is more to learn about cell size control, particularly for large cells and during post-Start budded growth.

We reasoned that size control could be better understood through the study of 'giant' budding yeast—cells prepared at sizes much larger than wildtype, which could subsequently be released into cell cycle progression. Such an approach could reveal whether large cells are subject to size regulation, as well as test for specific size control mechanisms (sizers, adders or timers) by identifying invariant parameters of growth (daughter size, interdivision volume, or budding duration, respectively). We thus pursued two molecular strategies to reversibly generate giant yeast: optogenetic disruption of the cell polarity factor Bem1 (Chenevert et al., 1992; Jost and Weiner, 2015) and a temperature-sensitive allele of the cyclin-dependent kinase Cdk1/Cdc28

(Reed and Wittenberg, 1990). Both perturbations prevented bud emergence but did not arrest cell growth, leading to cell sizes that were at least 10-fold larger than unperturbed cells. Upon release from their block, giant mothers reentered the cell cycle and populations of their progeny returned to their unperturbed size within hours. We found no evidence for an adder operating across the entire cell cycle in giant yeast, but our observations revealed a size-invariant timer that specifies the duration of S/G2/M across the full range of daughter sizes. Our data thus provide evidence that cell size homeostasis is maintained by at least two separable mechanisms of size control: a pre-Start size sensor enabling size-dependent passage through Start, and a post-Start timer ensuring that daughters are smaller than their mothers. Together, these mechanisms ensure that yeast populations generated from cells at either size extreme rapidly return to a set-point within only a few cell division cycles.

RESULTS AND DISCUSSION

Preparing 'giant yeast' *via* isotropic cell growth

To achieve reversible control over cell size in *S. cerevisiae*, we first took advantage of an optogenetic tool that utilizes the light-responsive PhyB/PIF system (Levskaya et al., 2009) to control the localization of Bem1, a cell polarity factor (Chenevert et al., 1992; Jost and Weiner, 2015). In this "optoBem1" system, red light illumination re-localizes the PIF-Bem1 fusion protein to mitochondrion-localized PhyB (**Fig. 1A**). Since PIF is fused to endogenous Bem1, light-induced Bem1 relocalization induces an acute loss-of-function phenotype where cells fail to form a site of polarized Cdc42 activity, fail to initiate budding, and instead undergo continuous isotropic growth (Jost and Weiner, 2015) (**Fig. 1B-C**). Strikingly, this effect is quickly reversed upon illumination with infrared (IR) light, which releases PIF-Bem1 from the mitochondria within seconds. Upon the switch to IR light, cells form a bud within minutes and proceed to cytokinesis (**Fig. 1, B and D**). Moreover, the PIF-Bem1 fusion protein appears to fully recapitulate normal Bem1 function: when it is not sequestered to the mitochondria, overall cell sizes and cell growth rates are similar to an isogenic wildtype strain (Jost and Weiner, 2015).

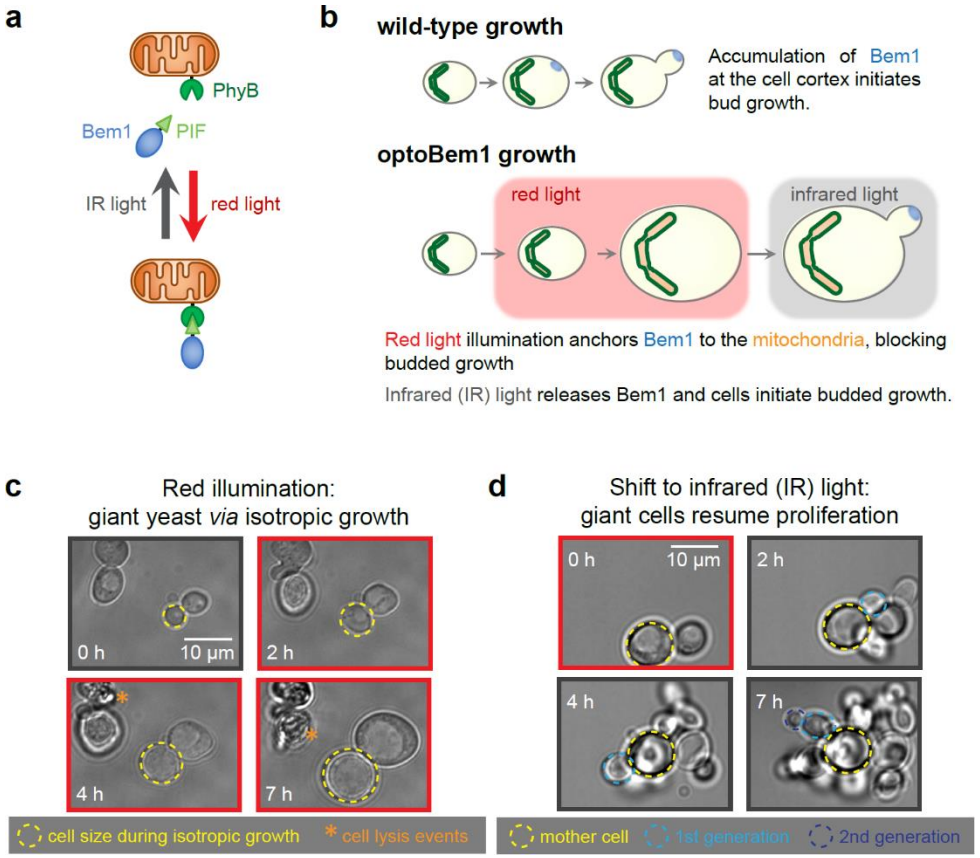

Figure 1. Control of yeast cell size using optogenetics.

(a) Exogenous PhyB (phytochrome B; dark green) is fused to the C-terminus of *S. cerevisiae* Tom20, anchoring it to the mitochondria outer membrane (orange). PIF (phytochrome-interacting factor; light green) is fused to endogenous Bem1 (blue). Illumination with red light drives a conformational change in PhyB allowing it to bind PIF-Bem1. Conversely, illumination with infrared (IR) light drives the reverse reaction, releasing PIF-Bem1.

(b) Top row. Bem1 (blue) localization to the plasma membrane is required for bud emergence and polarized growth. Bottom row. Illumination of yeast with red light sequesters Bem1 to the mitochondria (orange), preventing it from localizing to the plasma membrane to initiate budding. Yeast continue to grow isotropically while under red light. Illumination of yeast with IR light releases Bem1 from the mitochondria, allowing it to promote budding.

(c) Cells were illuminated with red light for 8 h (indicated by red borders) and imaged every 10 min using bright-field microscopy.

(d) Following red light illumination for 6-10 hours as in **1C**, large cells were illuminated with IR light (indicated by grey borders) and imaged every 5-10 min using bright-field microscopy.

We performed additional experiments to more completely characterize optoBem1 giant cells. Our initial experiments quantifying the growth of red light-illuminated optoBem1 cells revealed two subpopulations of cells that grew at different rates (**Fig. S1A**). We hypothesized that cell growth rates differed depending on the cell cycle phase at the time of Bem1 disruption. Indeed, we found

that synchronizing optoBem1 cells before red light stimulation led to unimodally-distributed growth (**Fig. S1B-C**). Furthermore, restricting our analysis to measure growth only following entry into G1 yielded a unimodal distribution (**Fig. S1D-H**). We also observed that a substantial fraction of optoBem1 yeast burst as they become increasingly large (**Fig. 1C**, asterisks; (Jost and Weiner, 2015)), and hypothesized that cell lysis may be a result of large cells' increased susceptibility to osmotic pressure. Supporting this hypothesis, growing cells in high-osmolarity media containing 1 M sorbitol decreased the frequency of cell lysis (**Fig. 2A**) without affecting the rate of isotropic growth (**Figs. 2B and S1A**). We therefore supplemented our media with sorbitol for all subsequent experiments involving optoBem1-arrested cells. Finally, to confirm that growth was indeed isotropic during the entire time period, we briefly incubated cells with fluorescent Concanavalin A (FITC-ConA) to mark the existing cell wall, followed by a washout of free FITC-ConA. We found that cells exhibited uniform dilution of FITC-ConA around their surface, suggesting that growth was indeed isotropic **(Fig. 2C)**. Collecting multiple z-plane images at high resolution revealed that cells maintained a spherical shape over a 12 h growth period, consistent with isotropic growth.

In budding yeast, the rate of isotropic growth during G1 is proportional to cell surface area

Prior studies have established that unperturbed, freely-cycling budding yeast cells exhibit an exponential growth in volume over time (Soifer et al., 2016; Di Talia et al., 2007). However, most of this growth is localized to the bud, with only a minor contribution from the mother cell's isotropic growth during G1. Furthermore, the mode of growth may change depending on cell cycle phase (Goranov et al., 2009). We reasoned that the ability to prepare isotropically-growing yeast with volumes spanning an order of magnitude would permit high-quality measurements of this growth law, and potentially reveal processes that limit cell growth as size increases.

We imaged optoBem1 cells during red light illumination at multiple z-planes and wrote custom code to automatically measure cell diameter every 10 min over a 12 h period. Following entry into G1 after Bem1 arrest, we found that isotropically-growing optoBem1 cells exhibited a linear increase in cell diameter over time, corresponding to a rate of volume growth proportional to t^3 (**Fig. 2D**). Since these volume increases also show a strong correlation with protein content, as assessed by fluorescence (Di Talia et al., 2007) (**Fig. S1I**), our data suggest that the growth we observed primarily arises from increases in cell mass rather than cell swelling (e.g., water influx). This result is inconsistent with two classic models of cell growth: a constant growth law, where

volume increases linearly over time; and exponential growth, where the rate of growth is proportional to the cell's current volume. In contrast, a linear increase in cell diameter is the expected result for volume increasing in proportion to cell surface area (Supplemental Experimental Procedures). Surface area-proportional growth could arise if nutrient/waste exchange across the plasma membrane is a limiting factor for growth in large spherical cells (Turner et al., 2012).

We observed that red light-illuminated optoBem1 cells also exhibited a change in DNA content over time. While most cells maintained a ploidy of 2N or less during the first 3 h of Bem1 disruption, a population of 4N cells appeared following 6 h of arrest (**Fig. 2E**), consistent with prior reports suggesting that, after Bem1 disruption, some arrested cells eventually leak through the cell cycle block and undergo DNA endoreduplication (Bender and Pringle, 1991). To ensure that the surface area-proportional growth was not an artifact of increased ploidy, we set out to generate 'giant yeast' *via* a second, non-optogenetic method: disruption of Cdk1/Cdc28 using the temperature-sensitive allele *cdc28-13* (hereafter referred to as *cdk1-ts*). Unlike optoBem1 cells, nearly all *cdk1-ts* cells at the restrictive temperature arrest in G1 without undergoing further DNA replication (Reed and Wittenberg, 1990).

We found that *cdk1-ts* cells grown at the restrictive temperature to induce arrest in G1 also exhibited a linear increase in cell diameter, consistent with growth proportional to surface area (**Fig. 2F**). However, *cdk1-ts* were unable to maintain this rate of growth over the entire 12-h time-course: After reaching a volume of 500-700 μm^3 (6-7 h following the temperature shift), cell growth stalled (**Fig. S1J**). Taken together, our results from both optoBem1 and *cdk1-ts* cells indicate that the rate of isotropic cell growth during G1 is proportional to surface area over wide range of yeast cell sizes. DNA endoreduplication does not appear to affect this overall growth rate but may be required to sustain it beyond a critical cell size, giving rise to the robust continued growth of optoBem1 cells. Indeed it has been shown in other organisms that DNA content scales with cell size in this manner (Edgar and Orr-Weaver, 2001). Our findings can be reconciled with the usual observation of exponential growth in wildtype budding yeast in at least two ways. First, exponential growth might only govern bud growth, masking a distinct growth law that operates in isotropically-growing cells. Second, it is possible that cells become surface area-limited at sizes just above that of wildtype cells, thereby inducing a shift from volume-proportional growth to surface area-proportional growth.

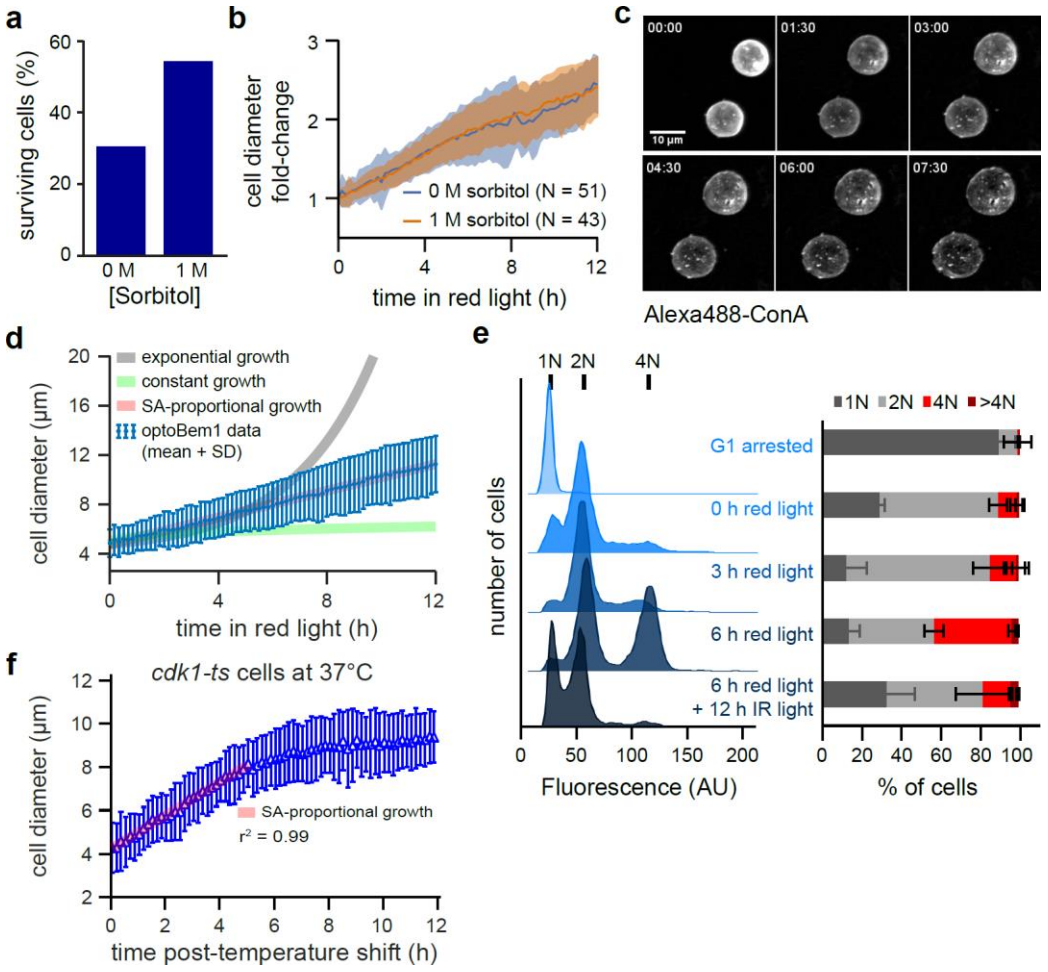

Figure 2. Effects of continuous isotropic growth on yeast physiology.

(a) Yeast were prepared and imaged as in **Fig. 1C-D** with media containing indicated concentrations of sorbitol. Each bar indicates the percentage of cells surviving the entire 12-h timecourse.

(b) Average normalized dimeter of yeast grown in media with or without 1 M sorbitol. N > 40 cells for each condition. Error bars, SD.

(c) Cell wall staining. Cells were prepared as in **2A**, treated with 100 µg/mL Alexa488-labeled concanavalin-A, and imaged every 15 min for 8 h. Each panel is a max intensity projection of multiple focal planes acquired via confocal microscopy. Yeast grow isotropically following Bem1 deactivation.

(d) Average growth trajectory for Bem1-arrested cells calculated as in **2B** for yeast in 1 M sorbitol from experiments described in **2A**. Each blue dot represents an average of 48 cells. Expected trajectories for exponential, constant, and surface-area-proportional growth are indicated by grey, green, and red lines, respectively.

(e) Cells were treated with red light for 6 hours, followed by 12 additional hours of IR light. Cells were collected, fixed, and stained with SYTOX Green at indicated timepoints following treatment with red or IR light. 'G1-arrested' cells were treated with alpha-factor for 3 h to arrest cells in G1, with a ploidy of 1N. Representative plots, left; averaged data from 2 independent experiments, right. Error bars, SD.

(f) Average growth trajectory for *cdk1-ts* cells at 37 °C. The relationship between diameter and time remained linear for the first 5 h of growth (r^2 = 0.998), but growth rapidly stalled at later timepoints. N = 126 cells.

Giant yeast retain size homeostasis

Cell size control pathways exist to correct for deviations from a set cell size, yet most previously-identified size control pathways specifically operate on cells that are born too small, delaying cell cycle progression to enable further growth to occur (Fantes, 1977; Kellogg, 2003). Because the light and temperature-shift stimuli with which we prepared 'giant' yeast are fully reversible, we reasoned that we could monitor the return to a steady-state size distribution after releasing giant cells from their block.

We prepared giant optoBem1 cells by incubating them in red light for 8 h and monitored them by live-cell microscopy after releasing them into infrared light. Surprisingly, we found that cell populations rapidly returned to their unperturbed state (**Fig. 3A**), with individual daughter cells reaching the set-point volume in as few as three rounds of division (**Fig. S2A**). Return to the set-point size is not driven by cell shrinking, as giant mothers maintained their maximum volume over multiple rounds of budding (e.g., **Fig. 1D**). Instead, the giant mothers are eventually diluted out as successive generations are born, an effect that is especially prominent in cell populations at least 10 h post-Bem1 release (**Fig. 3A**). In these populations, size distributions have a single mode near the set-point volume but exhibit long tails towards larger volumes (**Fig. S2B**). Our observation that cell size recovers after only a few generations strongly supports the existence of size control acting on large cells and demonstrates that size homeostasis across a cell population is robust even to extreme increases in cell volume.

Convergence of cells to a set-point size does not rely on adder-based mechanisms.

Growth of unperturbed yeast has been reported to be consistent with an adder mechanism, such that cells add a constant, defined volume over the course of a full cell cycle (Soifer et al., 2016). However, a subsequent study argued that the adder behavior could arise as a consequence of independent regulation of pre- and post-Start events, without a requirement for the cell to keep track of its added volume across all cell cycle phases, and may fail under various perturbations (Chandler-Brown et al., 2017). To test whether adder-based mechanisms could account for size control in giant yeast, we quantified interdivision volume change in successive cell division cycles after releasing optoBem1 cells into infrared light. For this experiment we prepared optoBem1 cells that also expressed fluorescently-labeled septin rings (Cid et al., 2001), which enabled us to time

both bud emergence and cytokinesis and thus separate pre-Start and post-Start size regulation (**Fig. 3B-C**).

The 'adder' model predicts that the cell volume at division (v_d, which includes both the mother and bud compartments) should be proportional to cell volume at birth (v_b) with a slope of 1 (i.e. $v_d = v_b + \Delta$, where Δ represents the constant volume increment 'added' through one cell cycle (**Fig. 3B**, rightmost blue-shaded area)) (Soifer et al., 2016). Indeed, for unperturbed cells, we found that cell volume at division was linearly related to volume at birth with a slope of 1.19 (95% CI, 0.82-1.56) (**Fig. 3D**). However, we found that the adder model poorly explained the cell size relationships in our giant cells, where the volume at division was related to volume at birth with a slope of 1.73 (95% CI, 1.32-2.13) (**Fig. 3D**). This relationship was also evident when individual cells were tracked over time: the interdivision volume change, Δ, was positively correlated with the volume at birth (**Fig. 3E**). This size-dependent volume change occurred entirely during S/G2/M phase, as cells added a minimal volume during G1 that did not vary with cell size (**Fig. 3E**, grey curve). We also performed analogous experiments in *cdk1-ts* giant cells that were shifted back to the permissive temperature. These experiments revealed a similar relationship: large cells grew more than small cells, exhibiting a linear relationship between volume at division and volume at birth with a slope of 1.70 (95% CI, 0.96-2.44) (**Fig. 3D**). These results are broadly consistent with recent work showing that although size control in unperturbed cells resembles an adder-based mechanism, no mechanistic adder regulates volume addition across the entire cell cycle (Chandler-Brown et al., 2017). Our data also suggest that any size regulation limiting the growth of large cells is likely a consequence of regulation in S/G2/M, as growth during G1 is negligible.

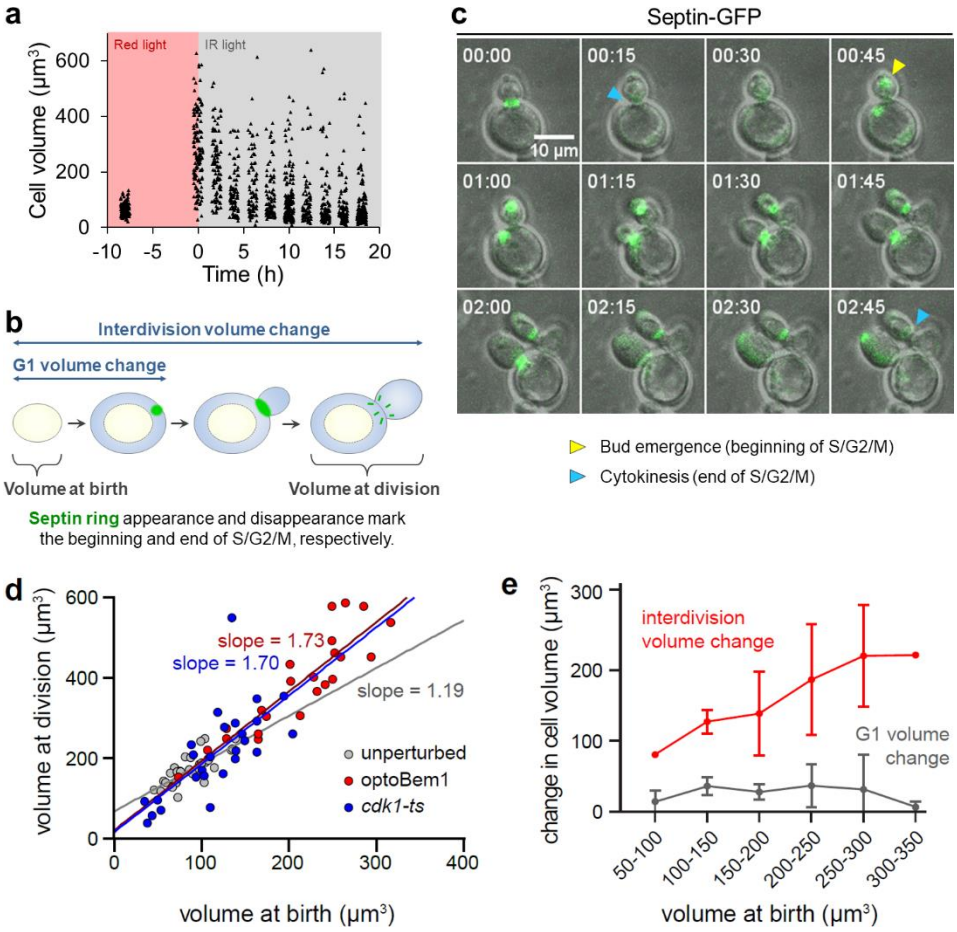

Figure 3. Convergence of yeast to set-point volume is inconsistent with an 'adder'.

(a) Cells were incubated under red light illumination for 8 h followed by IR light illumination for 18 h. At indicated timepoints (every 2 h during IR light illumination), cell volumes were measured by microscopy. Each point represents a single cell.

(b) Budding yeast cell cycle with labels depicting volume and growth intervals measured in **3C-E**. Blue-shaded areas, volume added as a newly-born cell grows.

(c) OptoBem1 cells were illuminated for 8-10 h with red light (to generate giant yeast), then switched to IR light (allowing giant yeast to bud and divide) and imaged every 5 min for ~8 h. *cdk1-ts* cells were incubated at 37 °C for 8 h, then switched to 25 °C prior to imaging. Exogenously-expressed Cdc10-GFP was used to mark septin rings (green). Panels depict representative optoBem1 cells. Time, HH:MM.

(d-e) Cells were imaged and analyzed as depicted in **3C**. "volume at birth" for daughters was measured when the septin ring separating the mother and daughter disappeared (e.g., **3C**, '00:15', blue arrowhead). "G1 volume change" is the difference between volume measured when bud emergence occurred in newly-born daughters (e.g., **3C**, '00:45', yellow arrowhead), and "volume at birth". "volume at division" was measured when daughters completed a subsequent round of cytokinesis (e.g., **3C,** '02:45', blue arrowhead) and included both the original daughter and her newly-formed bud. "interdivision volume change" is the difference between "volume at division" and "volume at birth". **(d)** Each point represents a single cell. Colored lines, best-fit line by linear regression analysis. **(e)** Cells were binned by volume at birth, as indicated. N = 28 optoBem1 cells.

A 'timer' specifying budding duration operates across a broad range of cell sizes.

If an adder is unable to explain size homeostasis in giant yeast, what regulatory mechanisms or growth laws might operate on the daughters of giant cells during S/G2/M? Two possibilities include a bud 'sizer', where bud growth would be restricted after reaching a critical size; and a bud 'timer' in which cytokinesis would occur after a fixed amount of time from the beginning of S/G2/M (i.e. bud emergence) (**Fig. 4A**). To distinguish between these possibilities, we tracked the timing of bud emergence and cytokinesis by septin ring appearance and disappearance, respectively, following reactivation of Bem1 in giant optoBem1 cells (**Fig. S3A**). Daughter volume strongly correlated with mother volume (**Fig. 4B**), inconsistent with a bud sizer mechanism. Our prior observation that the interdivision volume change scales positively with cell birth size (**Fig. 3E**) further argues against a bud sizer for cell volume control. In contrast, our data were consistent with a timer specifying the duration of S/G2/M: the time from bud emergence to cytokinesis did not vary as a function of mother cell volume and took average 95 min across cells of all volumes (**Fig. 4C**).

Similar experiments performed using *cdk1-ts* cells (**Fig. 4B-C**) were consistent with our observations in optoBem1 cells, revealing a size-independent duration of budding. However, we observed one notable difference: the duration of the size-invariant bud timer in giant *cdk1-ts* cells was substantially longer (215 min) than that of giant optoBem1 cells (95 min) (**Fig. 4C**). As Cdk1 promotes efficient mitosis (Reed and Wittenberg, 1990), the increased duration of the bud timer may arise from the need of *cdk1-ts* cells to synthesize fresh Cdk1 to complete S/G2/M following a shift from the restrictive to permissive temperature. Furthermore, even when grown at the permissive temperature, the doubling time of *cdk1-ts* cells is longer than an isogenic wildtype strain (**Fig. S3B**), suggesting that *cdk1-ts* may not be able to fully complement *CDK1*.

In sum, we find that a timer specifying a constant budding duration describes how a cell population founded by 'giant' cells returns to their set-point volume. Although mother and daughter sizes are correlated across a broad size range, daughters are always born smaller than mother cells. After cytokinesis, daughter cells remaining larger than the set-point volume exhibit a G1 phase with virtually no growth (**Fig. 3E**) and bud rapidly, leading to a geometric shrinking in successive generations (**Fig. 3A**). Indeed, a back-of-the-envelope calculation demonstrates that if newly-budded daughters are each 50% smaller than their mothers, a 32-fold decrease in cell volume can be achieved in 5 generations ($2^5 = 32$). Assuming a 100 min doubling time (**Fig. 4C**), a return

to the set-point size would take ~8 h. A fixed budding time, even in the absence of active molecular size sensors in S/G2/M, is sufficient to buffer against abnormally large cell sizes. We also note that the bud duration timer we describe is quite complementary to G1-phase size sensors such as Whi5 (Schmoller et al., 2015), which compensate for a small size at birth by elongating G1 phase.

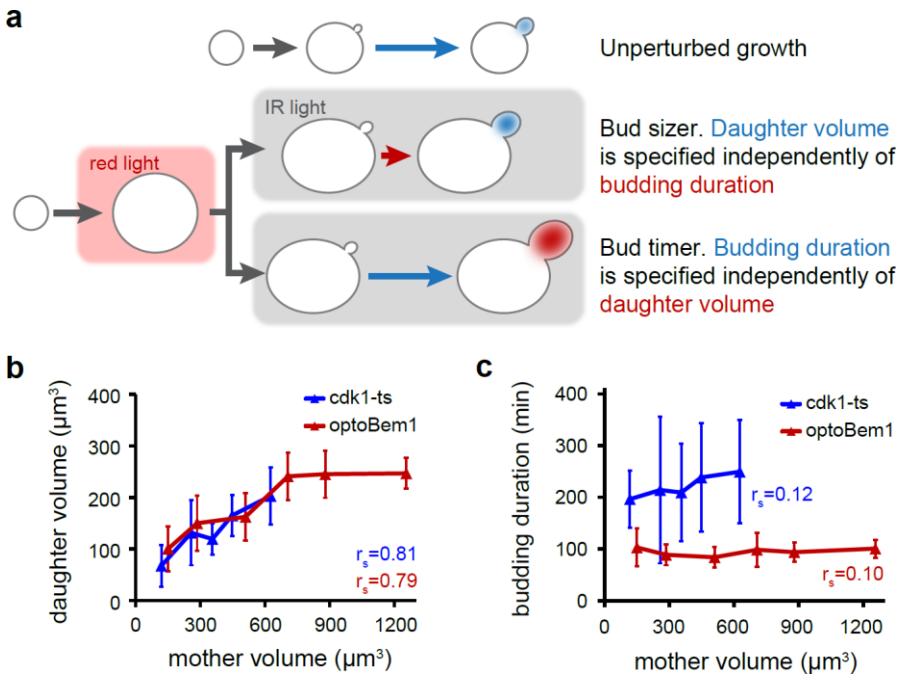

Figure 4. Comparison of sizer and timer mechanisms for regulation of bud growth.

(a) Schematic depicting the use of our optogenetics system for discriminating between bud 'sizer' and bud 'timer' mechanisms for specifying daughter cell volume.

(b and c) Cells were binned by mother volume in 200-µm increments. The average volume within each bin is plotted. Measurements of 'budding duration', 'mother volume', and daughter volume' were obtained as described in **Fig. S3A**. N = 73 optoBem1 cells and 80 *cdk1-ts* cells, with each bin containing at least 5 cells. Error bars, SD. r_s, Spearman's rho.

Our conclusions are derived from cells prepared using two independent perturbations: optogenetic inactivation of the Bem1 polarity factor and a temperature-sensitive Cdk1 kinase. Importantly, each of these perturbations targets distinct cellular processes and thus produces distinct physiological defects. Cells lacking Bem1 activity exhibit weakened cells walls (**Fig. 1C**) and undergo successive rounds of DNA endoreduplication following their initial arrest in G1 (**Fig. 2E**). In contrast, loss of Cdk1 does not produce such defects but its disruption requires incubating cells at 37 °C, which may broadly activate environmental stress response pathways. Furthermore, *cdk1-ts* may not fully complement *CDK1*, even at the permissive temperature (**Fig. S3B**). That

each of these perturbations reveals similar mother-daughter size correlations as well as a size-invariant bud timer strongly supports the generality of our conclusions.

The bud timer we describe here need not be a dedicated biochemical circuit to sense budding duration, compare it to a set-point, and dictate the transition to cytokinesis. Its existence could simply arise due to the time required by independent cellular processes that coincide with bud growth, such as the combined duration of S-phase or mitosis. Nevertheless, one observation suggests more complex regulation: the duration of the size-invariant bud timer is markedly longer in enlarged *cdk1-ts* vs. optoBem1 cells (**Fig. 4C**), yet mother-daughter sizes are nearly the identical in these two backgrounds (**Fig. 4B**). These data suggest that the duration of the bud timer may be inter-related to Cdk1 activity and cells' growth rate during S/G2/M. Recent work has found that mitosis and bud growth rate are closely coordinated and that cells may extend the duration of mitosis to compensate for slow growth that occurs under poor nutrient conditions (Leitao and Kellogg, 2017). Dissecting the dependencies between growth rate, Cdk1 activity and the duration of post-Start events presents a promising direction for future study.

MATERIALS AND METHODS

Strains, plasmids, and growth conditions. All yeast strains used are isogenic to an 'optoBem1' strain which was created in the w303 genetic background and contained exogenous PhyB-mCherry-Tom7 with endogenous Bem1 C-terminally tagged with mCherry-PIF, as previously described (Jost and Weiner, 2015). The *cdc28-13* (*cdk1*-ts) strain was a kind gift from David Morgan. A pACT1-CDC10-eGFP expression vector was created by Gibson assembly (Gibson et al., 2009), with the CDC10 expression cassette inserted between the NotI and XmaI sites of the pRS316 vector (Sikorski and Hieter, 1989). For the experiments described in **Figs. 3-4**, **S1D-G, and S2**, the indicated vector was transformed into our optoBem1 or *cdk1*-ts strain and selection was maintained by growing yeast in synthetic complete media lacking uracil (Sunrise). For all other experiments, yeast were cultured in synthetic complete media (Sunrise).

Preparation of giant yeast. Preparation of yeast prior to optogenetic experiments was performed, in general, as previously described (Jost and Weiner, 2015). Yeast undergoing exponential growth in synthetic media (with or without 1 M sorbitol) were treated with 31.25 μM phycocyanobilin (PCB; Santa Cruz Biotechnology, Inc.) and incubated in foil-wrapped tubes (to

block light) at 30 °C for a minimum of 2 h. For all microscopy experiments, yeast were spun onto glass-bottom 96-well plates (Brooks) coated with Concanavalin A and washed once with fresh PCB-containing media (with or without sorbitol) to remove floating cells. Cells remained approximately spherical following this procedure, as assessed by Concanavalin A staining (e.g., **Fig. 2C**). Mineral oil (Sigma-Aldrich) was then carefully layered on top of each sample to prevent evaporation. Imaging was performed at room temperature. For experiments where isotropic growth was measured (e.g., **Fig. 2A**), yeast were plated and imaged immediately following PCB treatment. For experiments where growth following Bem1 reactivation was examined (e.g., **Fig. 3**), PCB-treated yeast were first placed in clear culture tubes and incubated at room temperature for >6 h while undergoing constant illumination with a red LED panel (225 Red LED Indoor Garden Hydroponic Plant Grow Light Panel 14W, HQRP). Cells were then plated and imaged.

For experiments involving the *cdk1-ts* strain, cells were maintained in liquid cultures of synthetic complete media at 25 °C for at least 24 h and plated as described for the optoBem1 strain. Imaging was performed at 37 °C for experiments where isotropic growth during G1 was measured (e.g., **Fig. 2F**). For experiments where size control was assessed (e.g., **Fig. 4B-C**), cells were incubated at 37 °C for 8 hr, then shifted to 25 °C 30 min prior to imaging.

Microscopy. For isotropic growth experiments, samples were imaged on a Nikon Eclipse Ti inverted microscope equipped with a motorized stage (ASI), a Lamba XL Broad Spectrum Light Source (Sutter), a 60x 1.4 NA Plan Apo objective (Nikon), and a Clara interline CCD camera (Andor). Samples were imaged by bright-field microscopy every 10 min for 12 h. Throughout experiments involving optoBem1 cells, a red LED panel (HQRP) was carefully balanced against the motorized stage and microscope body to provide oblique illumination to the cells and ensure that Bem1 remained deactivated. Generous amounts of lab tape (Fisher) were applied to the LED panel and scope to prevent slippage during image acquisition and stage movement.

For the remaining experiments, samples were imaged on one of two spinning disk confocal microscopes, both of which were Nikon Eclipse Ti inverted microscopes with motorized stages (ASI). The first microscope was equipped with a Diskovery 50-µm pinhole spinning disk (Spectral Applied Research), a laser merge module (LMM5, Spectral Applied Research) with 405, 440, 488, 514, and 561-nm laser lines, a 60x 1.49 NA TIRF Apo objective (Nikon), and a Zyla sCMOS camera (Andor). The second microscope was equipped with CSU-X1 spinning disk (Yokugawa), a MLC400B monolithic laser combiner (Agilent) with 405, 488, 561, and 640-nm laser lines, a 60x

1.4 NA Plan Apo objective (Nikon), and a Clara interline CCD camera. All microscopes were controlled using Nikon Elements.

For experiments where Bem1 was reactivated following 8 h of deactivation, images were acquired every 5 or 10 min. During imaging, a 725-nm longpass filter (FSQ-RG9, Newport) was placed in the transmitted light path (gently resting on top of the condenser). The shutter for the transmitted light source was then left open for the entire duration of the experiment (even when images were not actively being acquired), such that cells were constantly illuminated with IR light, ensuring that Bem1 remained 'activated'. However, the shutter was briefly closed during acquisition of Cdc10-GFP images to reduce background.

Image Analysis. Cell volumes for yeast undergoing isotropic growth (i.e., **Figs. 2B, 2D, 2F, and S1**) were measured using custom Matlab code (available upon request) where a Hough transform was applied to bright-field images to identify cell boundaries. Cell radii were determined by calculating the geometric mean of the major and minor axes of the resulting ellipse. "cell diameter fold-change" (e.g., **Fig. 2B**) was determined by calculating the ratio of the cell diameter at each timepoint to the initial diameter of the cell at "0 h". A small fraction of cells did not arrest bud growth following Bem1 or Cdk1 inactivation and these were omitted from analysis. For cells growing and dividing following Bem1/Cdk1 reactivation (i.e., **Figs. 3, 4, and S2**) cell volumes were calculated by manually fitting ellipses to the cell boundaries with a single focal plane passing through the center of the cell. The major and minor axes of the ellipses were then determined, and cell volumes were calculated by solving for the volume of a prolate spheroid. For analysis of bud 'sizer' and bud 'timer' mechanisms (**Fig. 4B-C**), we included in our analysis mother cells that had previously been Bem1- or Cdk1-deactivated. These cells were omitted from our analysis of total volume addition over the course of an entire cell cycle (**Fig. 3**), given that we had strongly perturbed their growth during G1 following Bem1 or Cdk1 disruption. For the experiments depicted in **Fig. 3D**, all Bem1- and Cdk1-disrupted cells were from the same generation: daughters produced by giant mothers following Bem1 or Cdk1 reactivation. "Unperturbed" cells in **Fig. 3D** indicate optoBem1 cells that were grown in the absence of PCB (i.e. Bem1 activity was not light-responsive). A small fraction of both optoBem1 and *cdk1-ts* giant cells failed to bud following reactivation of Bem1 or Cdk1 and these were omitted from analysis. All cells quantified were obtained from two independent experiments, unless stated otherwise in the figure legends.

Quantification of protein levels. To determine cellular protein levels in growing yeast, we quantified mCherry fluorescence in our cells, which expressed *BEM1-mCherry-PIF* under the endogenous *BEM1* promoter and *PhyB-mCherry-CAAX* under the *ADH1* promoter, by spinning-disc confocal microscopy. Isotropic growth was induced as described in the "Preparation of yeast for optogenetic experiments" section. Cells were imaged 6 h following optogenetic-based Bem1 deactivation. Z-stacks containing 51 slices with 0.5 µm spacing with the shutter remaining open between each z-step were then collected. Sum projections were created from the entire stack, corrected for uneven illumination, and processed to remove background. Fluorescence intensity was measured from whole-cell regions-of-interest using ImageJ. Cell volume was approximated by measuring the major and minor axis of each cell and using these values to solve for the volume of a prolate spheroid.

Flow cytometry to measure ploidy. PCB-treated cells were placed in clear culture tubes and incubated at room temperature while undergoing constant illumination with a red LED panel. Samples (200 µL each) were collected at 0, 3, and 6 h following illumination with red light. The remainder of the culture was then placed under an IR LED (740-nm, Lightspeed Technologies) for an additional 12 h, after which a final sample was collected. Upon collection, cells were immediately treated with 475 µL 100% ethanol and fixed for 1 h at room temperature. Cells were then pelleted, washed once with 50 mM sodium citrate (pH = 7.2), and then resuspended in 500 µL 50 mM sodium citrate (pH = 7.2) to which RNaseA (0.25 mg/mL) had been added. Following an incubation for 1 h at 37 °C, 50 µL proteinase K was added to a final concentration of 2 mg/mL and cells were incubated at 50 °C for an additional hour. SYTOX green was then added to each sample to a final concentration of 2 µM, and cells were incubated for 1 h at room temperature. In parallel, control samples were prepared containing exponentially growing cultures of yeast treated with α-factor (10 µg/mL) for for ~3 h prior to fixation and staining. Ploidy was determined by measuring the fluorescence intensity of SYTOX green staining by flow cytometry using a FACSAria III (BD Biosciences) and normalizing to the α-factor-treated samples, which have a ploidy of 1N. For each timepoint for each independent experiment, 50,000 cells were measured. Analysis of flow cytometry data was performed using FlowJo and Flowing Software (http://flowingsoftware.btk.fi).

Calculation of doubling times. Prior to each experiment, cells were grown overnight to saturation in synthetic complete media at 25 °C. Cells were then diluted to an OD_{600} of 0.5-1.0 in fresh media

and incubated while shaking in a Biotek H4 Plate Reader. The OD_{600} for each culture was measured every 5 min for 14-16 h, by which point growth curves reached saturation. Doubling times were then determined by plotting $\log_2(OD_{600})$ vs. time and calculating the slope over the linear portion of the growth curve. Each point indicates an independent experiment.

ACKNOWLEDGEMENTS

We thank Anna Payne-Tobin Jost for helpful discussions, Alba Diz-Muñoz for experimental assistance, Fred Chang for critical reading of the manuscript and Nairi Hartooni for reagents. We also thank the organizers of the 2015 MBL Physiology course, Wallace Marshall, Jennifer Lippincott-Schwartz, and Rob Phillips, as well as all the course staff for creating the well-run, intellectually-stimulating environment from which this project grew. Support for this work was provided by a Post-Physiology Course Award from the Marine Biological Laboratory to C.A.H.A., the Thomas B. Grave and Elizabeth F. Grave Scholarship to F.D., and the National Institutes of Health [GM118167 to O.D.W., DP2EB024247 to J.E.T., and T32HL773125 to B.R.G.].

AUTHOR CONTRIBUTIONS

Conceptualization, all authors; Software, F.D. and J.E.T.; Investigation, C.A.H.A, F.D., J.E.T., and B.R.G.; Writing – original draft, B.R.G.; Writing – review and editing, all authors.

REFERENCES

Amir, A. (2014). Cell size regulation in bacteria. Phys. Rev. Lett. *112*.

Amodeo, A.A., and Skotheim, J.M. (2016). Cell-Size Control. Cold Spring Harb. Perspect. Biol. *8*, a019083.

Bender, A., and Pringle, J.R. (1991). Use of a screen for synthetic lethal and multicopy suppressee mutants to identify two new genes involved in morphogenesis in Saccharomyces cerevisiae. Mol. Cell. Biol. *11*, 1295–1305.

Brooks, R.F., and Shields, R. (1985). Cell growth, cell division and cell size homeostasis in Swiss 3T3 cells. Exp. Cell Res. *156*, 1–6.

Cadart, C., Monnier, S., Grilli, J., Sáez, P.J., Srivastava, N., Attia, R., Terriac, E., Baum, B., Cosentino-Lagomarsino, M., and Piel, M. (2018). Size control in mammalian cells involves

modulation of both growth rate and cell cycle duration. Nat. Commun. *9*, 3275.

Campos, M., Surovtsev, I.V., Kato, S., Paintdakhi, A., Beltran, B., Ebmeier, S.E., and Jacobs-Wagner, C. (2014). A constant size extension drives bacterial cell size homeostasis. Cell *159*, 1433–1446.

Chandler-Brown, D., Schmoller, K.M., Winetraub, Y., and Skotheim, J.M. (2017). The Adder Phenomenon Emerges from Independent Control of Pre- and Post-Start Phases of the Budding Yeast Cell Cycle. Curr. Biol. *27*, 2774–2783.e3.

Charvin, G., Cross, F.R., and Siggia, E.D. (2009). Forced periodic expression of G1 cyclins phase-locks the budding yeast cell cycle. Proc. Natl. Acad. Sci. USA *106*, 6632–6637.

Chenevert, J., Corrado, K., Bender, A., Pringle, J., and Herskowitz, I. (1992). A yeast gene (BEM1) necessary for cell polarization whose product contains two SH3 domains. Nature *356*, 77–79.

Cid, V.J., Adamiková, L., Sánchez, M., Molina, M., and Nombela, C. (2001). Cell cycle control of septin ring dynamics in the budding yeast. Microbiology (Reading, Engl.) *147*, 1437–1450.

Conlon, I., and Raff, M. (2003). Differences in the way a mammalian cell and yeast cells coordinate cell growth and cell-cycle progression. J. Biol. *2*, 7.

Edgar, B.A., and Orr-Weaver, T.L. (2001). Endoreplication Cell Cycles. Cell *105*, 297–306.

Elliott, S.G., and McLaughlin, C.S. (1978). Rate of macromolecular synthesis through the cell cycle of the yeast Saccharomyces cerevisiae. Proc. Natl. Acad. Sci. USA *75*, 4384–4388.

Eun, Y.-J., Ho, P.-Y., Kim, M., LaRussa, S., Robert, L., Renner, L.D., Schmid, A., Garner, E., and Amir, A. (2018). Archaeal cells share common size control with bacteria despite noisier growth and division. Nat. Microbiol. *3*, 148–154.

Fantes, P.A. (1977). Control of cell size and cycle time in Schizosaccharomyces pombe. J. Cell Sci. *24*, 51–67.

Gibson, D.G., Young, L., Chuang, R.-Y., Venter, J.C., Hutchison, C.A., and Smith, H.O. (2009). Enzymatic assembly of DNA molecules up to several hundred kilobases. Nat. Methods *6*, 343–345.

Ginzberg, M.B., Kafri, R., and Kirschner, M. (2015). Cell biology. On being the right (cell) size. Science *348*, 1245075.

Godin, M., Delgado, F.F., Son, S., Grover, W.H., Bryan, A.K., Tzur, A., Jorgensen, P., Payer, K., Grossman, A.D., Kirschner, M.W., et al. (2010). Using buoyant mass to measure the growth of single cells. Nat. Methods *7*, 387–390.

Goehring, N.W., and Hyman, A.A. (2012). Organelle growth control through limiting pools of cytoplasmic components. Curr. Biol. *22*, R330–9.

Goranov, A.I., Cook, M., Ricicova, M., Ben-Ari, G., Gonzalez, C., Hansen, C., Tyers, M., and Amon, A. (2009). The rate of cell growth is governed by cell cycle stage. Genes Dev. *23*, 1408–

1422.

Gregory, T.R. (2001). Coincidence, coevolution, or causation? DNA content, cell size, and the C-value enigma. Biol. Rev. Camb. Philos. Soc. *76*, 65–101.

Hartwell, L.H., and Unger, M.W. (1977). Unequal division in Saccharomyces cerevisiae and its implications for the control of cell division. J. Cell Biol. *75*, 422–435.

Harvey, S.L., and Kellogg, D.R. (2003). Conservation of mechanisms controlling entry into mitosis: budding yeast wee1 delays entry into mitosis and is required for cell size control. Curr. Biol. *13*, 264–275.

Johnston, G., Pringle, J., and Hartwell, L. (1977). Coordination of growth with cell division in the yeast. Exp. Cell Res. *105*, 79–98.

Jost, A.P.-T., and Weiner, O.D. (2015). Probing Yeast Polarity with Acute, Reversible, Optogenetic Inhibition of Protein Function. ACS Synth. Biol. *4*, 1077–1085.

Kellogg, D.R. (2003). Wee1-dependent mechanisms required for coordination of cell growth and cell division. J. Cell Sci. *116*, 4883–4890.

Leitao, R.M., and Kellogg, D.R. (2017). The duration of mitosis and daughter cell size are modulated by nutrients in budding yeast. J. Cell Biol. *216*, 3463–3470.

Levskaya, A., Weiner, O.D., Lim, W.A., and Voigt, C.A. (2009). Spatiotemporal control of cell signalling using a light-switchable protein interaction. Nature *461*, 997–1001.

Lloyd, A.C. (2013). The regulation of cell size. Cell *154*, 1194–1205.

Marshall, W.F. (2011). Origins of cellular geometry. BMC Biol. *9*, 57.

McNulty, J.J., and Lew, D.J. (2005). Swe1p responds to cytoskeletal perturbation, not bud size, in S. cerevisiae. Curr. Biol. *15*, 2190–2198.

Pan, K.Z., Saunders, T.E., Flor-Parra, I., Howard, M., and Chang, F. (2014). Cortical regulation of cell size by a sizer cdr2p. Elife *3*, e02040.

Reed, S.I., and Wittenberg, C. (1990). Mitotic role for the Cdc28 protein kinase of Saccharomyces cerevisiae. Proc. Natl. Acad. Sci. USA *87*, 5697–5701.

Schmoller, K.M. (2017). The phenomenology of cell size control. Curr. Opin. Cell Biol. *49*, 53–58.

Schmoller, K.M., Turner, J.J., Kõivomägi, M., and Skotheim, J.M. (2015). Dilution of the cell cycle inhibitor Whi5 controls budding-yeast cell size. Nature *526*, 268–272.

Sikorski, R.S., and Hieter, P. (1989). A system of shuttle vectors and yeast host strains designed for efficient manipulation of DNA in Saccharomyces cerevisiae. Genetics *122*, 19–27.

Soifer, I., Robert, L., and Amir, A. (2016). Single-Cell Analysis of Growth in Budding Yeast and Bacteria Reveals a Common Size Regulation Strategy. Curr. Biol. *26*, 356–361.

Spoerl, E., Loveless, L.E., Weisman, T.H., and Balske, R.J. (1954). Studies on cell division. II. X-radiation as a division inhibiting agent. J. Bacteriol. *67*, 394–401.

Taheri-Araghi, S., Bradde, S., Sauls, J.T., Hill, N.S., Levin, P.A., Paulsson, J., Vergassola, M., and Jun, S. (2015). Cell-size control and homeostasis in bacteria. Curr. Biol. *25*, 385–391.

Di Talia, S., Skotheim, J.M., Bean, J.M., Siggia, E.D., and Cross, F.R. (2007). The effects of molecular noise and size control on variability in the budding yeast cell cycle. Nature *448*, 947–951.

Turner, J.J., Ewald, J.C., and Skotheim, J.M. (2012). Cell size control in yeast. Curr. Biol. *22*, R350–9.

Varsano, G., Wang, Y., and Wu, M. (2017). Probing Mammalian Cell Size Homeostasis by Channel-Assisted Cell Reshaping. Cell Rep. *20*, 397–410.

SUPPLEMENTARY MATERIALS

Figure S1. Characterization of temperature- or optogenetically-induced isotropic growth.

Figure S2. Volume measurements of daughter cells.

Figure S3. Growth rates of yeast strains.

Supplemental Experimental Procedures.

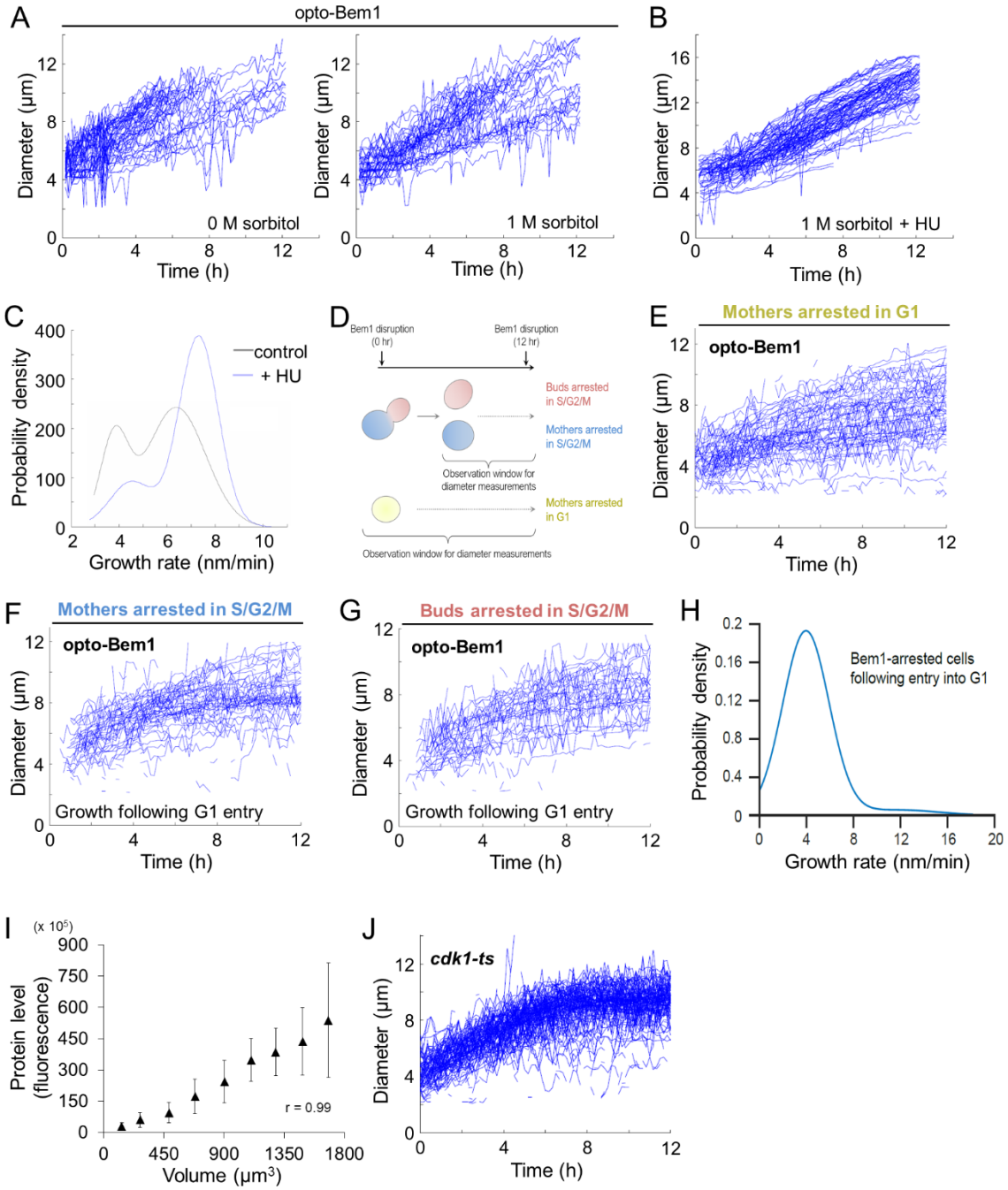

Figure S1. Characterization of temperature- or optogenetically-induced isotropic growth.

(A) Growth rates of single optoBem1 cells in synthetic complete media containing 0 M or 1 M sorbitol.

(B) OptoBem1 cells were prepared as in **2B** and synchronized in S-phase via incubation with 0.2 M hydroxyurea for 3 h followed by washout using media containing 1 M sorbitol.

(C) Probability distributions for growth rates measured in cells from **S1A**, right panel and **S1B**.

(D-G) Growth rates of single optoBem1 cells in synthetic media with 1 M sorbitol. Asynchronous populations of cells were treated with red light illumination to disrupt Bem1 and cells were grouped based on initial cell cycle stage as depicted in **(D)**: cells in G1 **(E)**, mothers in S/G2/M **(F)**, or buds in S/G2/M **(G)**. Growth rates for cells not already in G1 (i.e., **S1F-G**) were only measured following entry into G1, as indicated by these traces not beginning at '0 h' and as depicted in **S1D**.

(H) Probability distribution for growth rates of Bem1-disrupted cells following entry into G1 (i.e., **S1E-G**).

(I) Fluorescence of exogenously-expressed PhyB-mCherry-Tom7 under control of an ADH1 promoter was measured in cells of indicated volumes. Cells were binned by mother volume in 200-μm increments. The average volume within each bin is plotted. N = 300 cells. Error bars, SD. r, Pearson's correlation coefficient.

(J) Growth rates of single *cdk1-ts* cells at 37 °C. Cells were shifted from 25 °C to 37 °C 45 min prior to the start of the experiment to allow for Cdk1 disruption.

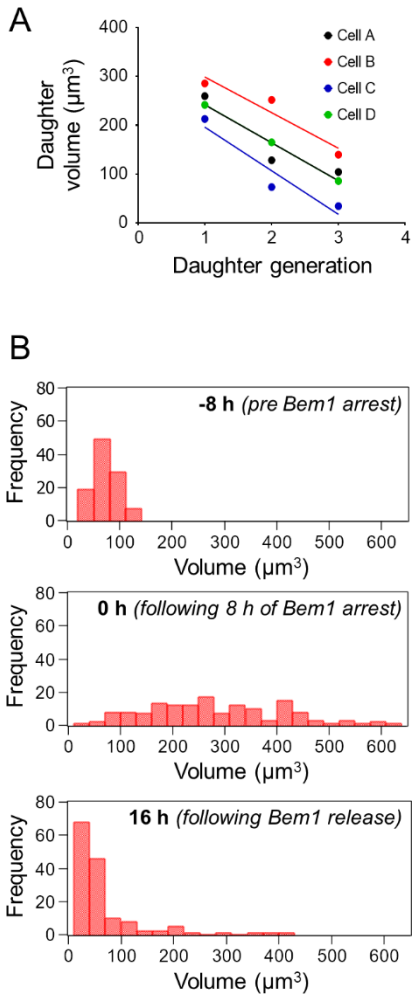

Figure S2. Volume measurements of daughter cells.

(A) Representative optoBem1 daughter cells from experiments in Fig. 4C-D. Only the daughters of daughters were measured for each generation.

(B) Histograms depicting cell volume distributions for indicated timepoints in **3A**.

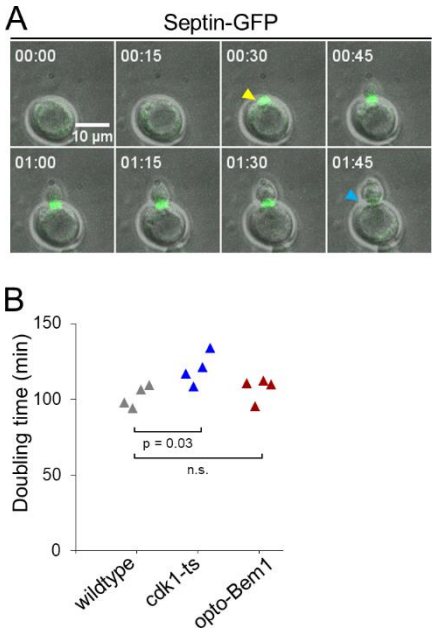

Figure S3. Growth rates of yeast strains.

(A) opto-Bem1 cells were illuminated for 6-8 h with red light (to generate giant yeast), then switched to IR light (allowing giant yeast to bud and divide). Similarly, *cdk1-ts* cells were incubated at 37 °C for 8 h (to generate giant yeast), then shifted to 25 °C (allowing giant yeast to bud and divide). All cells were imaged every 5-10 min for ~8 h. Exogenously-expressed Cdc10-GFP was used to mark septin rings (green) and measure cell cycle progression. Panels depict representative opto-Bem1 cells. Budding duration, difference between the time of division (e.g., septin ring disappearance at '01:45') and time of birth (e.g., septin ring appearance at '00:30'). 'Mother volume' was measured at the time of daughter cell birth (e.g., yellow arrow) and 'daughter volume' (i.e. only the former bud compartment) was measured at cytokinesis (e.g., blue arrow). Time, HH:MM.

(B) Bud growth rates following Bem1 release in opto-Bem1 yeast. Cells were binned by mother volume (i.e. not including the bud volume), as indicated, with each bin containing at least 6 cells. Error bars, SD. The average growth rate for buds of mothers "801 - 1400 μm^3", 4.62 μm^3/min, was significantly larger than the average growth rate of buds of mothers "0 - 400 μm^3", 2.46 μm^3/min ($p < 0.05$, Mann-Whitney U-test).

(C) Doubling times of indicated strains in liquid culture at 25 °C during log-phase growth.

Supplemental Experimental Procedures

1 Different models of growth

1.1 Growth proportional to surface area

We found that the radius r grows linearly with time t:

$$r(t) = at \tag{1}$$

where a is an arbitrary constant. It follows that

$$\frac{dr}{dt} = a \tag{2}$$

Ultimately, we are interested in how the volume changes over time ($\frac{dV}{dt}$) to be able to compare it with known growth models. We can calculate $\frac{dV}{dt}$ with the help of the known $\frac{dr}{dt}$ by:

$$\frac{dV}{dt} = \frac{dr}{dt}\frac{dV}{dr} \tag{3}$$

The volume and the radius are related by the formula for the volume of a sphere $V = \frac{4}{3}\pi r^3$. Calculating the derivative of the volume with respect to the radius

$$\frac{dV}{dr} = 4\pi r^2 = A \tag{4}$$

results in the expression for the surface area A of a sphere. Using equations (2) and (4) in (3) leads to

$$\frac{dV}{dt} = aA \tag{5}$$

This shows that if the radius grows linearly with time, the volume always grows proportionally to the surface area. Using the formulas for the surface area and the volume of a sphere, we see that plotting surface area over time would result in a quadratic curve, while the volume depends on time to the power of 3.

1.2 Growth proportional to volume

For comparison, we briefly describe what growth proportional to the volume would look like. Growth proportional to volume means that

$$\frac{dV}{dt} = aV \tag{6}$$

Solving this leads to

$$logV = at + C \tag{7}$$

where C is an arbitrary constant. Using the formula for the volume of a sphere, we can express the volume as a function of the radius:

$$log\left(\frac{4}{3}\pi r^3\right) = at + C \tag{8}$$

This can be rewritten as

$$\frac{4}{3}\pi r^3 = e^{at+C} \tag{9}$$

Solving for r leads to

$$r(t) = \left(\frac{3}{4\pi}\right)^{\frac{1}{3}} e^{\frac{1}{3}(at+C)} \tag{10}$$

This means that r would grow exponentially with time. The same is true for the surface area A and the volume (by using the expression for r in equation (10) in $A = 4\pi r^2$, $V = \frac{4}{3}\pi r^3$).

1.3 Constant growth

Another common model of growth is constant growth with respect to the volume, where

$$\frac{dV}{dt} = a \tag{11}$$

Solving this leads to

$$V = at + C \tag{12}$$

Including the volume as a function of radius

$$\frac{4}{3}\pi r^3 = at + C \tag{13}$$

leads to the following dependence of r on time t:

$$r(t) = \left(\frac{3(at+C)}{4\pi}\right)^{\frac{1}{3}} \tag{14}$$

This shows that in case of constant growth with respect to the volume, the radius would grow proportional to $t^{\frac{1}{3}}$, the surface area proportional to $t^{\frac{2}{3}}$, and the volume (as the name of this model says) proportional to t.